Prism Computational Sciences, Inc.
455 Science Drive, Suite 140
Madison, WI 53711

Modeling of Inner-Shell Kα and Kβ Line Emission from Germanium Dopants in Capsule Implosion Experiments

I. E. Golovkin, J. J. MacFarlane, P. R. Woodruff

Prism Computational Sciences, Inc.

PCS-R-131

September 2012

Table of Contents

1. Introduction

This report describes upgrades to the modeling of inner-shell line emission produced by x-ray photoionization of K-shell electrons in SPECT3D and PrismSPECT. This work is motivated by the presence of germanium (Ge) Kα and Kβ emission lines observed in Ge-doped capsule implosion experiments at NIF [1]. In these experiments, x-rays generated in the hot core of a compressed capsule are capable of photoionizing K-shell electrons of ions residing in the surrounding cooler shell. The K-shell vacancies can be quickly filled in by *2p→1s* (Kα) and *3p→1s* (Kβ) radiative transitions, thereby producing the observed emission lines.

During this reporting period, the atomic modeling in SPECT3D and PrismSPECT has been upgraded to include photoionization of K-shell (1s) electrons for ions having more than 10 electrons (Na-like and lower ionization stages of Ge). For ions with fewer than 11 bound electrons, the atomic models in the Prism Atomic Physics Data Library include a sufficient number of atomic levels and transitions involving K-shell vacancies that atomic processes and spectra can be accurately computed. For ions with a relatively large number of bound electrons, we use a different approach because of the potentially very large number of states that need to be considered in the atomic modeling. In this case, a set of autoionization levels with K-shell vacancies can be automatically added to the atomic model based on the "thermal" (*i.e.,* non-autoionizing) levels selected for a simulation. For example, a K-shell electron of the Ti-like state $1s^2 2s^2 2p^6 3s^2 3p^6 3d^4$ can be removed to create the autoionizing state $1s^1 2s^2 2p^6 3s^2 3p^6 3d^4$. This level can in turn decay radiatively into $1s^2 2s^2 2p^5 3s^2 3p^6 3d^4$ and give rise to Kα line emission from the Sc-like ion. We sometimes refer to these states with inner-shell vacancies as *virtual autoionization states* (or VAS levels) because these levels are not explicitly included in the atomic physics database.

The VAS modeling in SPECT3D and PrismSPECT has been used in simulating Cu Kα and Kβ emission that is observed in short-pulse laser experiments [2,3]. In this case, autoionization states for a wide variety of ions can be populated as energetic electrons eject K-shell electrons via electron-impact ionization. In the NIF capsule implosion experiments, however, x-rays originating in the hot core photoionize K-shell electrons in the cooler, moderately ionized Ge that resides in the surrounding shell. We note that it is important to include the effects of K-shell photoionization for each of the thermal level in the atomic model that is significantly populated.

In this report, we show sample results from simulations which utilize the updated modeling and discuss results relevant to recent ICF capsule implosion experiments involving Ge-doped ablators. The spectra observed in these experiments are of significant value because they are used to infer the amount of shell material that gets mixed into the hot core in the experiments. Because of this, accurate modeling and interpretation of the spectra is important.

2. Simulation of Ge Kα/Kβ Emission in Capsule Implosion Experiments

Figure 1 displays an example spectrum obtained in a NIF capsule implosion experiment [1]. The experiments were designed to infer fuel-pusher mix information based on Ge spectral signatures. The emission signatures from Ge can be summarized as follows:

- strong emission from Ge "cold" Kα ($h\nu$ = 9.9 keV) and He-α ($h\nu$ = 10.28 keV);
- significant emission from satellites to the He-α due to $2p \rightarrow 1s$ transitions originating from L-shell ionization stages (*e.g.*, Li-like through B-like Ge) at $h\nu$ ~ 10.0 - 10.25 keV;
- weak Ly-α emission at $h\nu$ ~ 10.6 keV;
- weak emission from He-β + satellites from L-shell ionization stages at $h\nu$ ~ 11.7 - 12.2 keV.

We note that "cold" Kβ emission for Ge has a wavelength of $h\nu$ ~ 11.0 - 11.1, and therefore was not observed in the experimental spectrum shown in Figure 1.

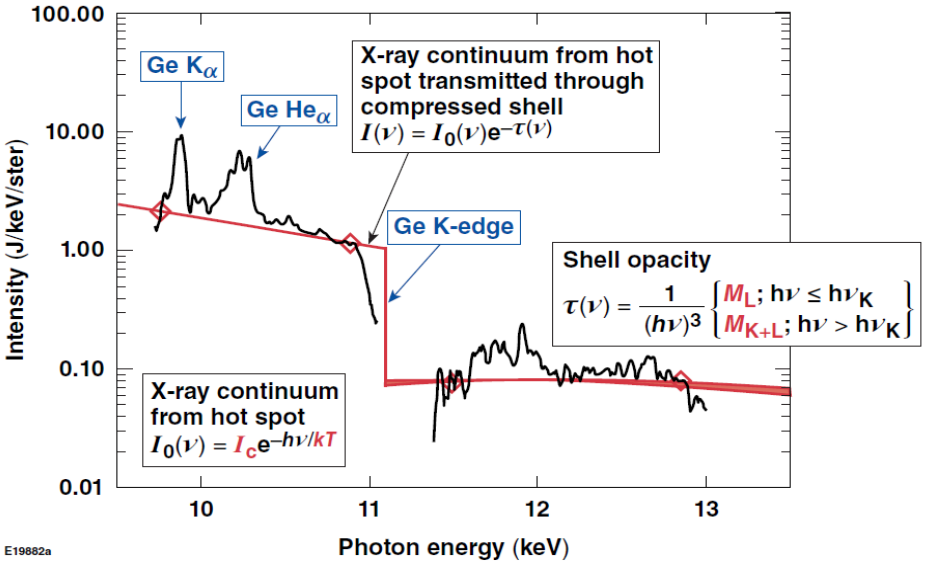

Figure 1. Ge K-shell emission spectrum obtained in NIF capsule implosion experiment (from Ref. [1]).

It is believed that the "cold Kα" emission is produced as relatively cold Ge in the shell is photoionized by x-rays originating in the hot core. Photoionization of K-shell electrons in low-to-moderate ionization stages of Ge requires photons with energies of $h\nu \gtrsim 11.0$ keV. We note that at photon energies of ~ 9.5 - 11 keV the observed x-ray spectrum is clearly dominated by Ge emission (as opposed to either free-free or bound-free emission from carbon or hydrogen isotopes). It seems likely that Ge is also the dominant source of emission at photon energies above 11 keV, arising mainly from Kβ and He-β emission lines of Ge. Thus, it is likely photons originating from hot Ge in the

core produce the K-shell photoionization of relatively cool Ge in the shell, which in turn gives rise to the observed Kα observed at $h\nu \sim 9.9$ keV. That is, there is a link between the amount of Ge that gets mixed into the hot core, and the amount of Kα line radiation that is observed.

2.1. SPECT3D Simulations with Simple Plasma Grid

Because of this potential link between the emission observed from the hot and cool regions, we performed a series of SPECT3D simulations using a simple spatial grid that is composed of both hot and cool regions. In our baseline set of simulations, we used a 1-D spherically symmetric plasma with four regions:

- unmixed hot dense DT fuel at $T = 2.5$ keV;
- a "hot mix" region at either $T = 1.5$ keV or $T = 2.0$ keV, where the Ge ionization is dominated by K-shell ions (H, He, Li-like);
- a dense "cool mix" region at $T = 200$ eV, where Ge ionization is dominated by Ge XI – Ge XIV (Ti-like through K-like Ge);
- a cooler, lower density undoped CH ablator region.

The CH ablator was doped with 1% Ge (by number). The mix region was assumed to be 90% DT fuel and 10% CH ablator. Figure 2 shows an example the radial dependence of the electron temperature, mass density, and electron density across all regions.

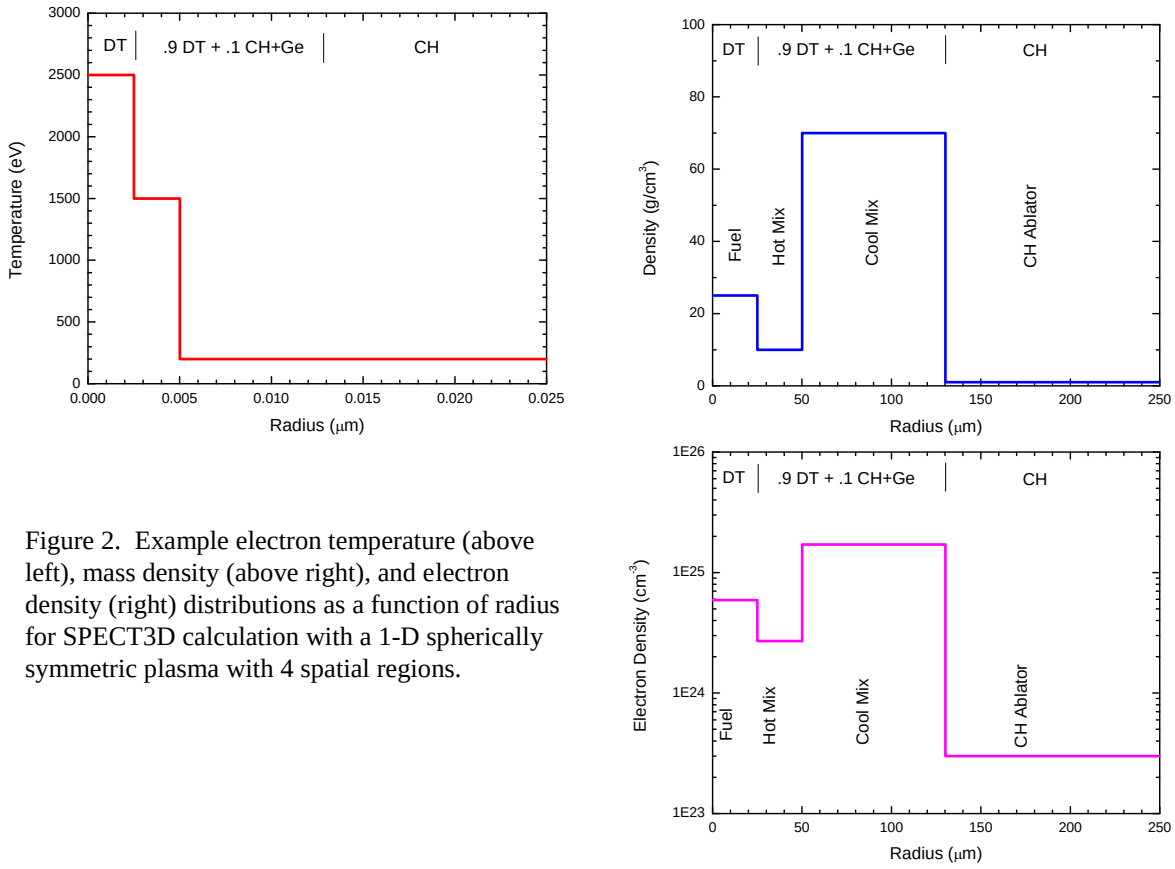

Figure 2. Example electron temperature (above left), mass density (above right), and electron density (right) distributions as a function of radius for SPECT3D calculation with a 1-D spherically symmetric plasma with 4 spatial regions.

For this density distribution, the total Ge mass in the hot mix region is 110 ng.

Figure 3 (red curve) shows the emission spectrum computed for the 4-region plasma grid discussed above using the updated photoionization modeling in SPECT3D. Note that many of the gross characteristics of the computed spectrum are consistent with the experimental spectrum shown in Figure 1, including the strong emission from cold Kα and He-α, satellites to the low-energy side of the He-α line (*i.e.*, at $h\nu \sim 10.0$ - 10.25 keV), and He-β emission lines that are between one and two orders of magnitude lower in intensity than the Kα and He-α lines.

To examine the role of hot core photons in producing cold Kα and Kβ emission, we performed an additional SPECT3D simulation in which photoionization was neglected for all transitions. Figure 3 (blue curve) shows that in the absence of photoionization, the cold Kα and Kα does not appear in the spectrum.

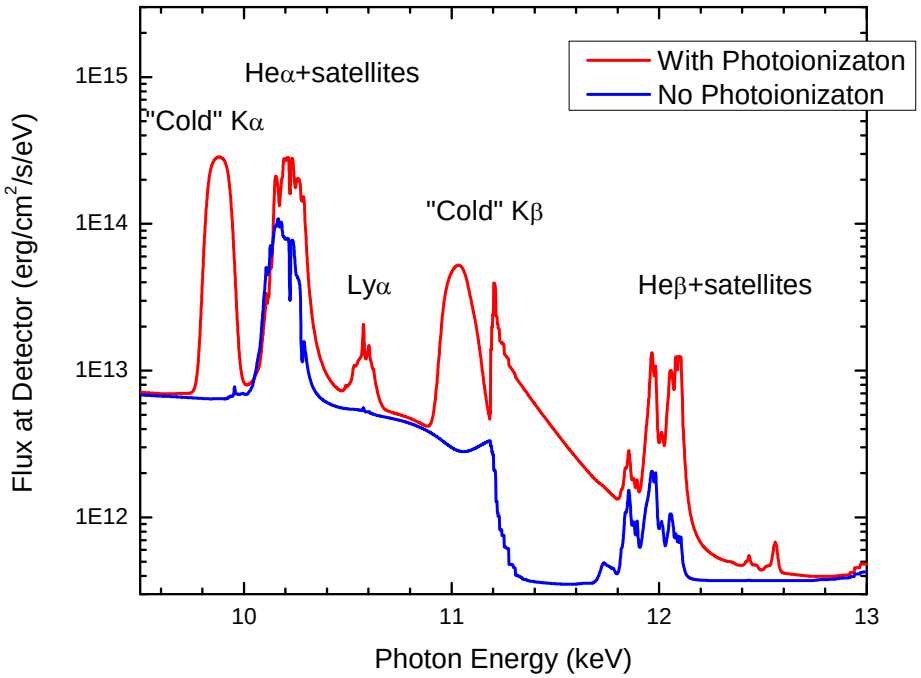

Figure 3. Calculated space-integrated Ge emission spectra for nominal case with T = 2.0 keV. Red curve: Photoionization is included. Blue curve: Photoionization is neglected. If photoionization is not included in the calculation, the emission signatures from colder region are not present.

The number of Ge emitters in the hot region affects not only the intensity of the "thermal" K-shell line emission (*i.e.*, Li-, He-, and H-like line emission that is produced by electron collisions and is typically seen in laser-produced plasmas), which originates in the hot mix region of the 4-region plasma grid, but also affects the intensity of the cold Kα and Kβ line emission. This is shown in Figure 4, where spectra computed using different concentrations of Ge in the ablator are shown. The results show that the

intensity of cold Kα/Kβ emission increases with the increasing concentration of Ge. By decreasing the concentration of Ge from 1.0% to 0.1% in both the hot mix and cool mix regions, the intensity of the cold Kα and Kβ emission lines decreases by more than an order of magnitude. This decrease is caused by both the decrease in the number of Ge ions in the cool mix region (which produce the cold Kα emission), and the number of photons originating in the hot mix region. Note that because of resonant self-absorption effects, the hot emission escaping the hot mix region is not linearly proportional to the concentration of Ge.

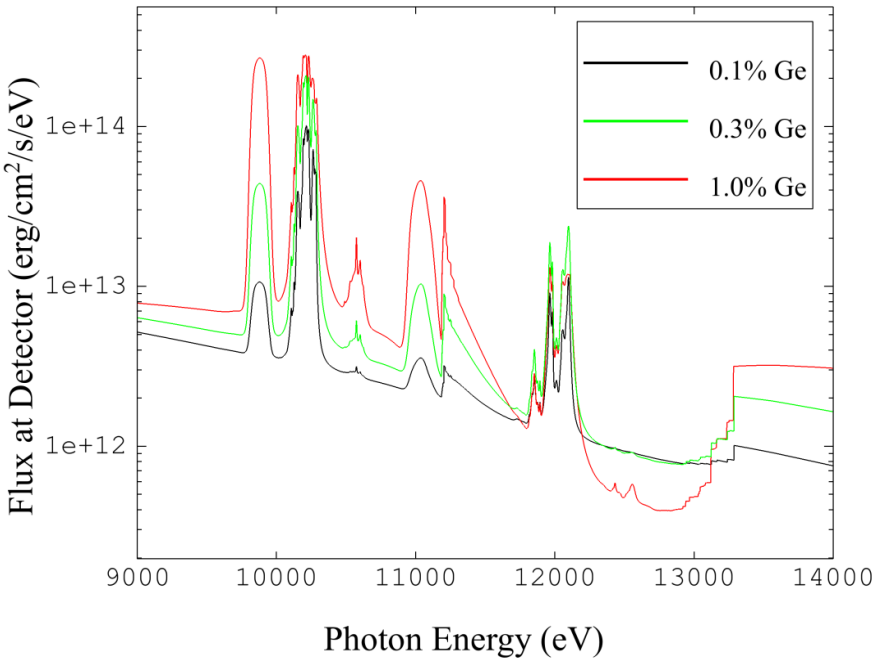

Figure 4. Space-integrated emission spectra compute for different Ge concentrations in the ablator of the 4-region plasma grid.

The intensity of He-α line and its satellites are subject to opacity effects. This is because the ionization stages producing this emission have electronic configurations containing *2p* vacancies. This is shown in Figure 5, where the frequency-dependent optical depth for a line-of-sight (LOS) going through the center of the spherical plasma grid is shown for various concentrations of Ge. Note that the optical depths for the strongest lines range up to ~ 10^2 for the highest concentration case. On the other hand, the cold Kα optical depths are small because the ionization stages producing this emission have electronic configurations with filled *2p* subshells. Because of this, the relative intensity of the cold Kα lines increases with respect to the resonance He line as Ge concentration increases.

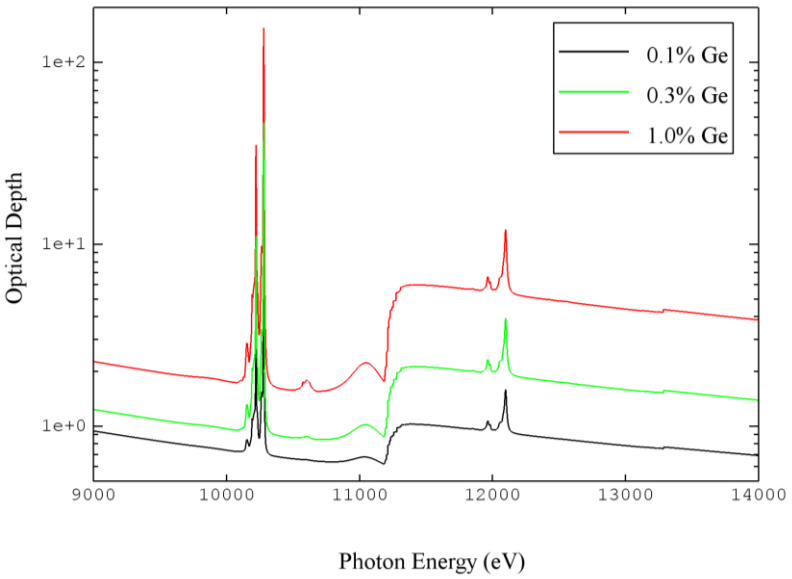

Figure 5. Ge optical depths compute for different Ge concentrations for the 4-region plasma grid.

Figure 6 shows which regions of the spherical plasma grid contribute to the various spectral characteristics. The red curve corresponds to the intensity for a line-of-sight that extends through the center of the grid. Note that this LOS shows contributions from both the cold Kα/Kβ features and the hot line emission (*i.e.*, He-α, He-β and satellites). By comparison, LOSs that miss the hot mix region include emission only from the cold Kα/Kβ features.

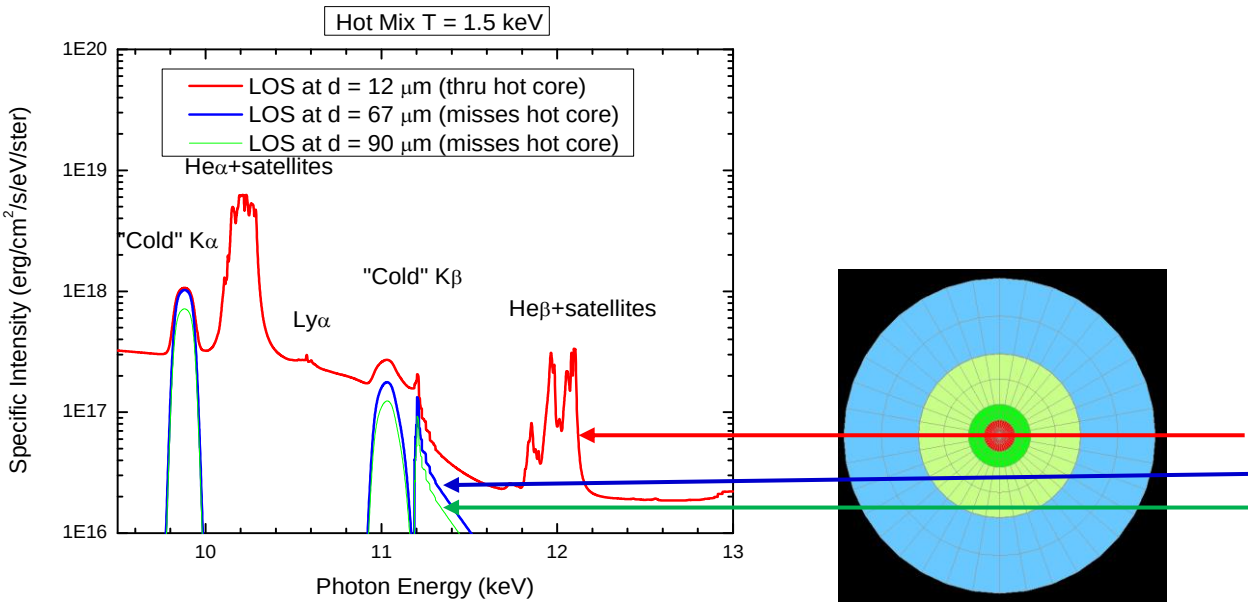

Figure 6. Ge spectral intensites corresponding to various lines-of-sight extending through the plasma grid.

Figure 7 shows the sensitivity of the Ge line intensities to the temperature of the hot mix region. As the temperature of the hot mix region decreases from 2.0 to 1.5 keV, the emission from the hot region decreases, which in turn causes the emission from the cold Kα/Kβ features to decrease. Thus, it is clear that the absolute intensity of the line emission observed in the experiments is sensitive to the temperature of the hot mix region.

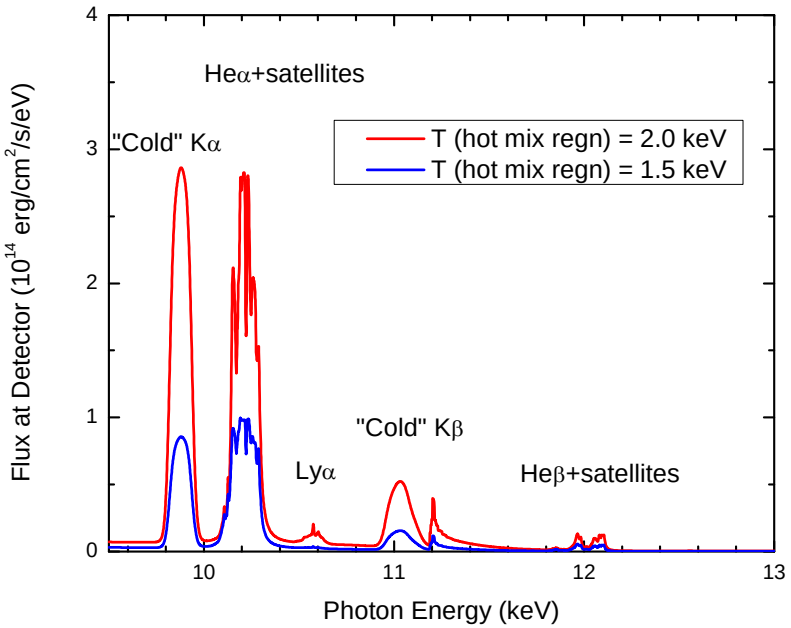

Figure 7. Ge emission spectra computed for 4-region plasma grid. Red curve: Nominal case with a hot mix region temperature of 2.0 keV. Blue curve: Case with hot mix temperature of 1.5 keV.

The cold Kα feature originates in the cold mix region and is produced when photons with energies above K edge ($h\nu \gtrsim 11$ keV), originating in the hot mix region, photoionize *1s* electrons from Ge ions of relatively low ionization stage (*i.e.*, ions with filled L shells). To assess the contribution from the various potential radiation sources from the hot mix region, we performed additional calculations in which: (1) no Ge was in the hot mix region, and (2) the only emission contributing to the radiation field above 11 keV was free-free emission. Figure 8 compares results from the nominal case (red curve) with the no Ge in hot region case (black curve) and free-free only at $h\nu \gtrsim 11$ keV case (green curve). Note that when only free-free emission is allowed to contribute to the radiation field at photon energies above 11 keV, there is a non-trivial amount of emission from cold Kα, but the overall intensity is down by approximately an order of magnitude compared to the nominal case. The primary source of the free-free emission is free electrons from the dominant species in the plasma (*i.e.*, DT and CH, which are fully ionized). This suggests that most of the photons that produce the cold Kα originate from Ge transitions within hot mix region.

The above 4-region plasma grid model, while simplistic, helps provide insights into the physical processes that affect the observed Ge spectra.

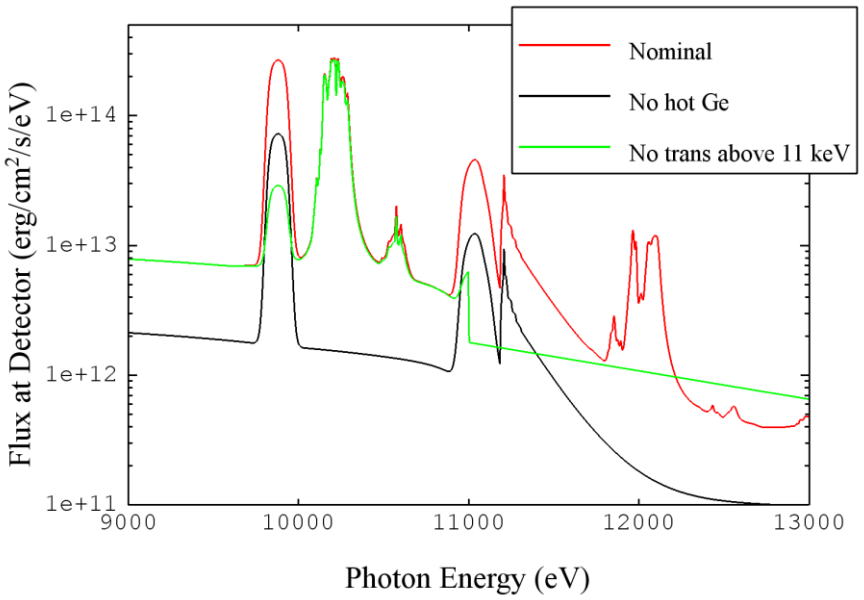

Figure 8. Photopumping of cold K-alpha transitions is driven by energetic photons from hot Ge.

2.2. PrismSPECT Simulations

Next, we present results from PrismSPECT calculations (*i.e.*, single volume element calculations) which show the sensitivity of emission spectra to plasma conditions. In these simulations, the plasma is composed of 90% DT, 9.9% CH, and 0.1% Ge (by number), and has a characteristic size of 25 microns. We also include an external radiation field with a T = 2.5 keV (blackbody). Figure 9 shows the mean charge state computed for Ge as a function of temperature for two different densities. Ionization varies significantly across the range of conditions.

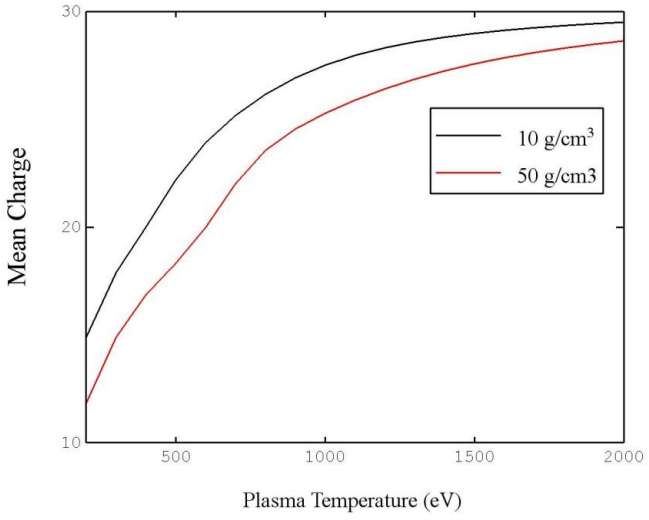

Figure 9. Mean charge state of Ge in a DT/CH mixture as a function of temperature for two densities.

Figure 10 shows Kα and Kβ spectra computed using PrismSPECT for different temperatures at a mass density of 10 g/cm^3. Note that at lower temperatures, the dominant features shift towards longer wavelengths as they originate from lower ionization stages. Figures 11 through 15 show the contribution from various ionization stages of Ge at plasma temperatures ranging from 500 eV to 2,000 eV.

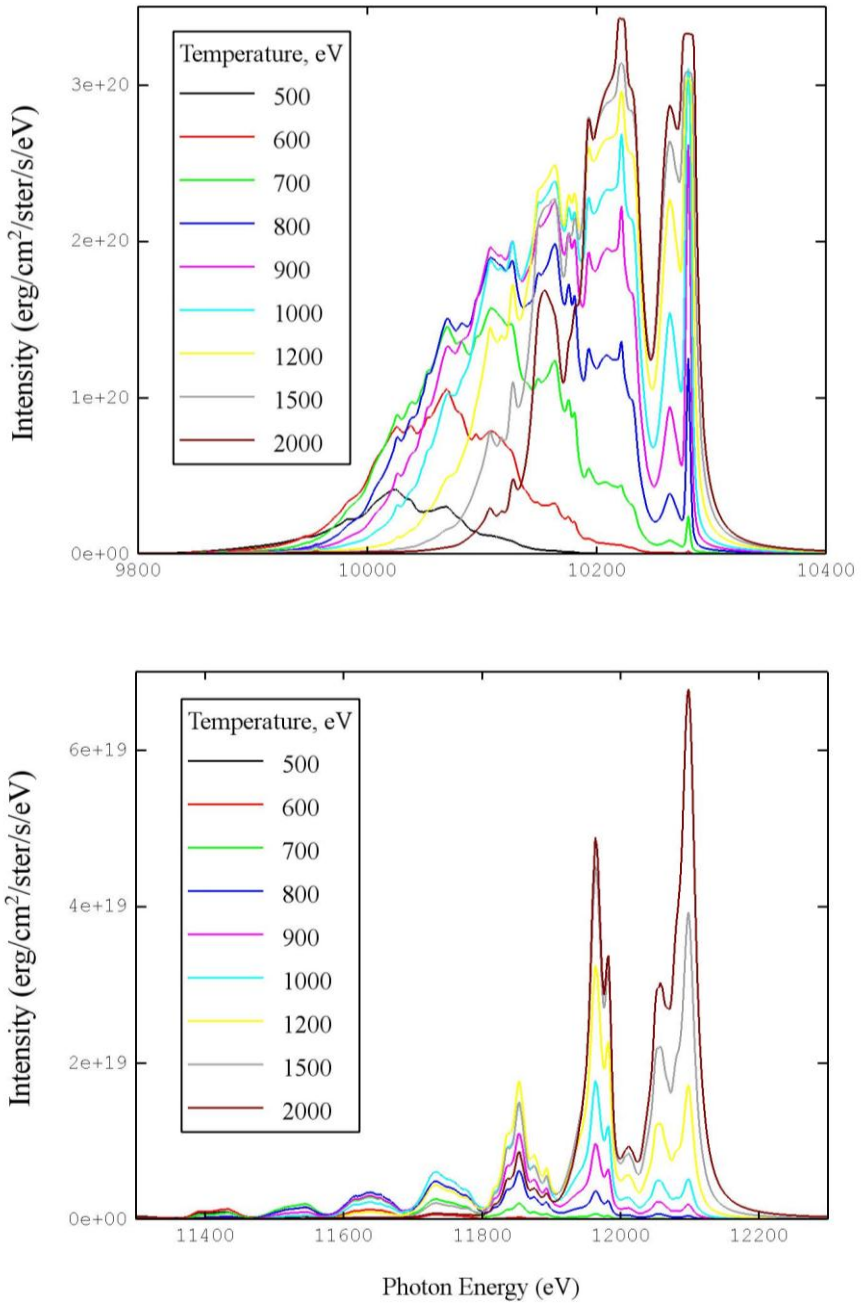

Figure 10. Spectra for Kα (top) and Kβ (bottom) transitions computed for different temperatures using PrismSPECT.

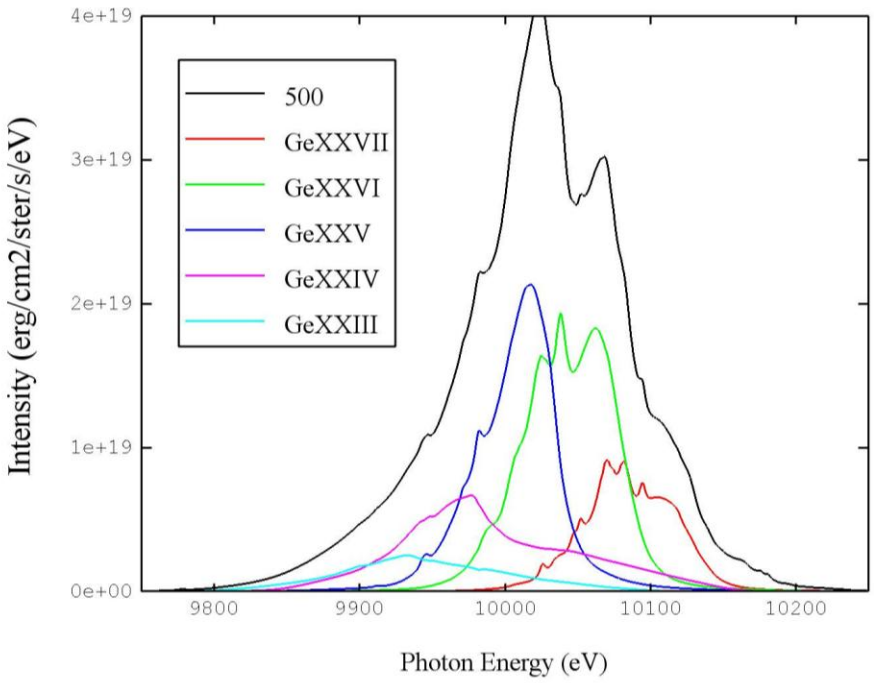

Figure 11. Calculated spectrum and contributions from various ionizations for Kα transitions computed at T = 500 eV.

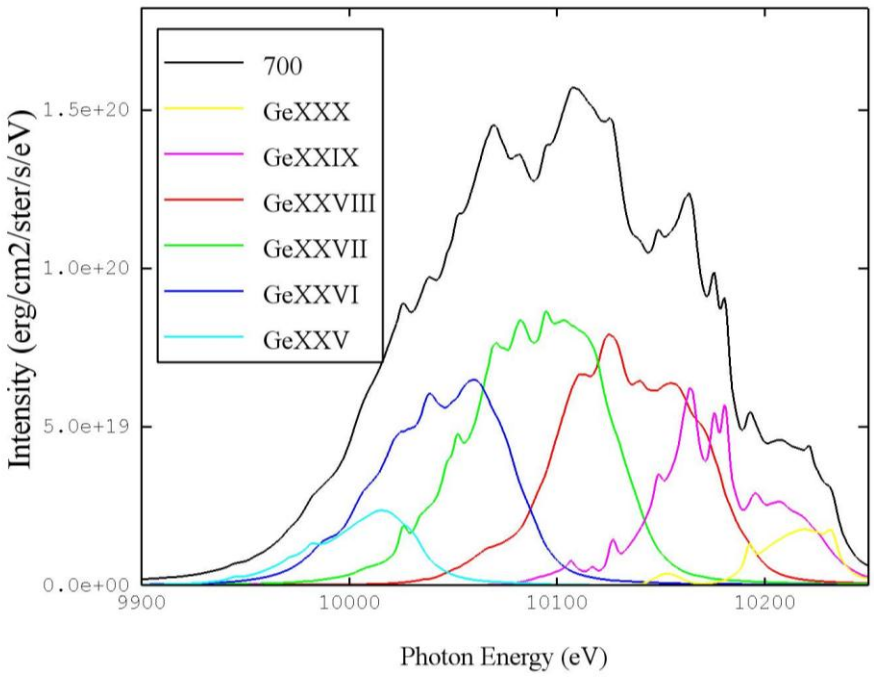

Figure 12. Same as Fig. 11, but at T = 700 eV.

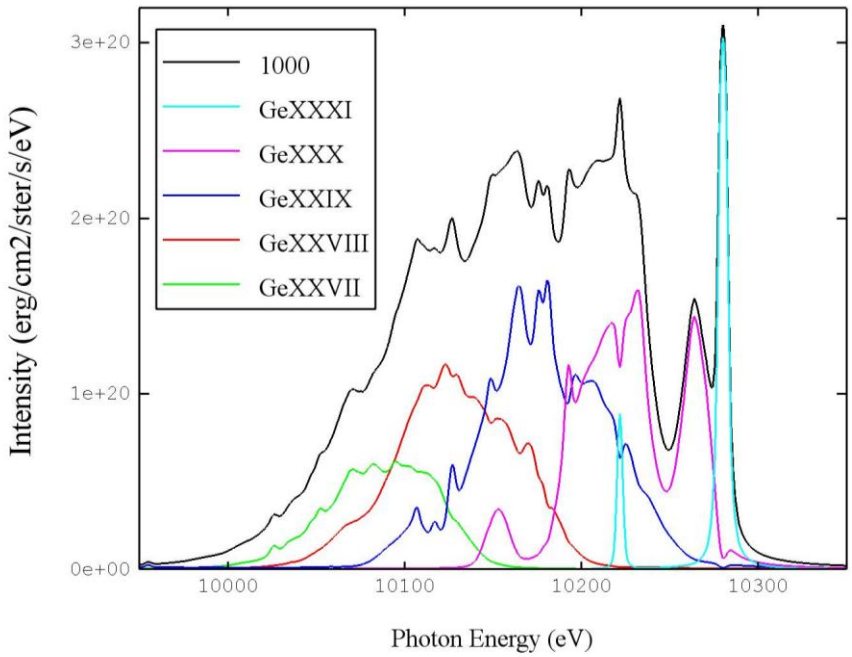

Figure 13. Same as Fig. 11, but at T = 1000 eV.

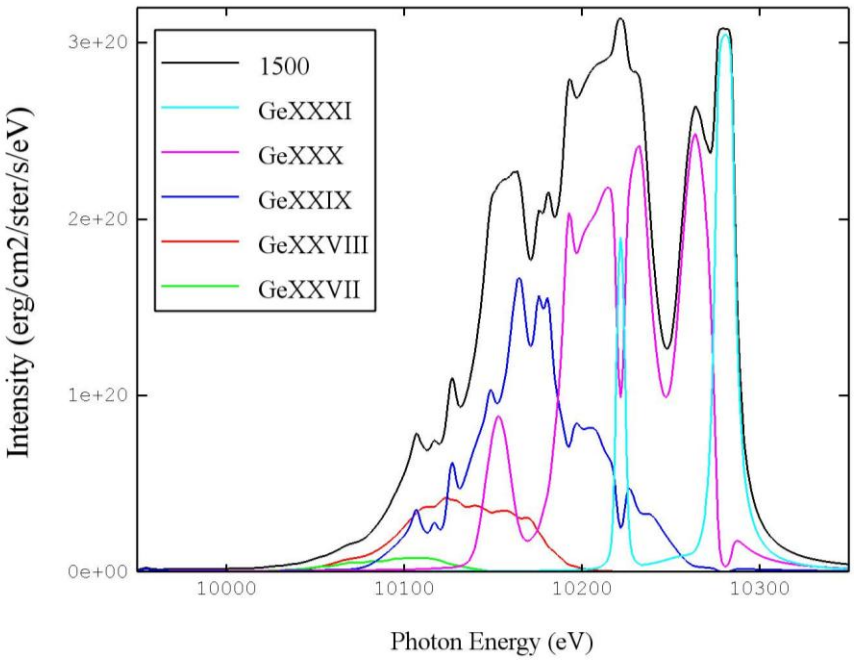

Figure 14 Same as Fig. 11, but at T = 1200 eV.

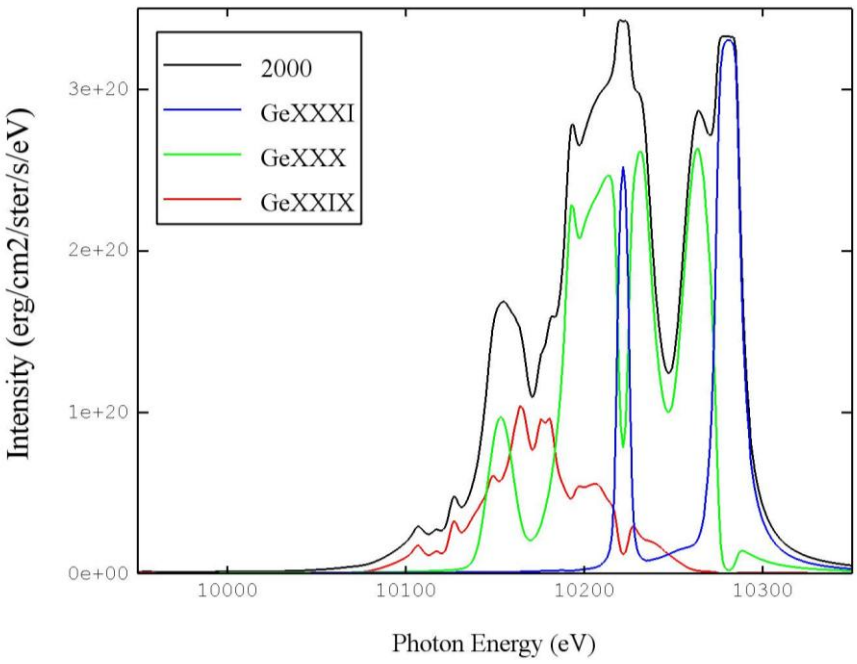

Figure 15. Same as Fig. 11, but at T = 2000 eV.

Figure 16 shows the frequency-dependent optical depths at several temperatures. At these temperatures, significant ionization of Ge L-shell electrons occurs. As vacancies appear in the *2p* subshell, resonant self-absorption in the Kα lines becomes possible.

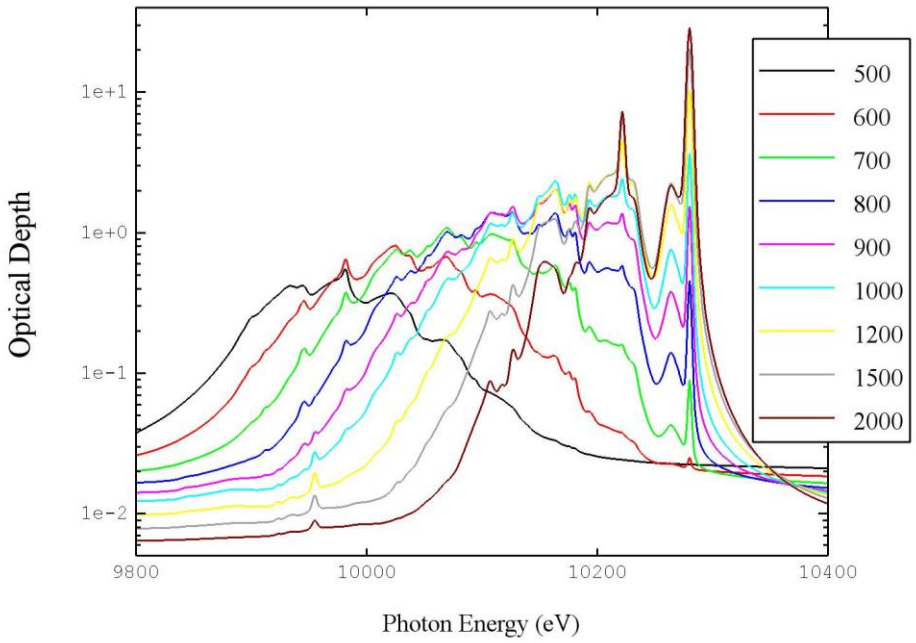

Figure 16. Optical depth for α transitions computed for different temperatures.

2.3. SPECT3D Simulations with Plasma Gradients

Finally, we present results of SPECT3D calculations which utilize electron temperature and density distributions which have smooth gradients in the mix region. The distributions are plotted in Figure 17 as functions of distance along a line-of-sight that goes through the plasma center. Other simulation parameters are the same as in the simple 4-region case of hot/cold mix regions.

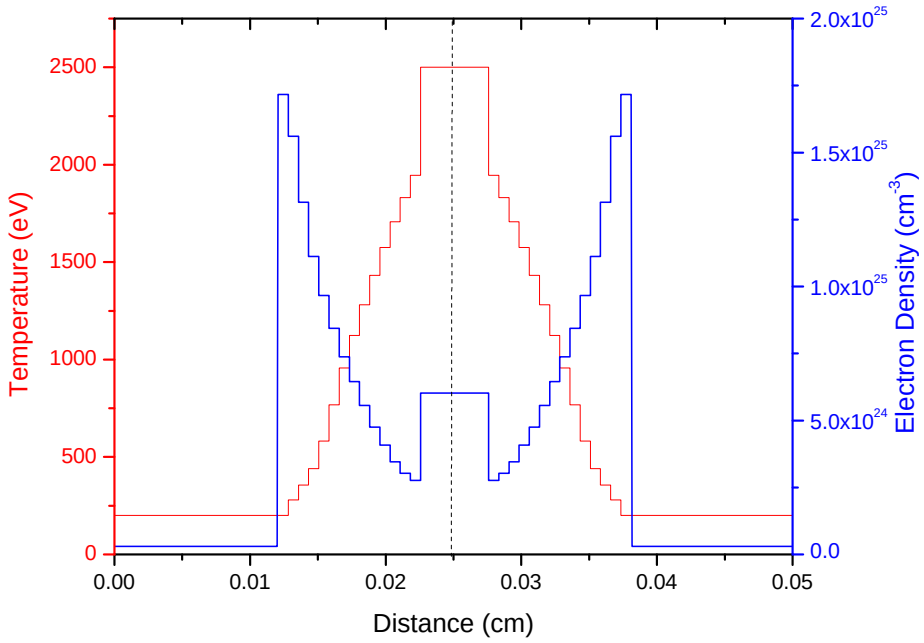

Figure 17. Electron temperature and density distribution in SPECT3D simulation.

Because of the smooth gradients, we can expect a broad distribution of Ge ionization stages to be present in the mix region which contribute to the overall emission spectrum. Figure 18 shows results comparing spectra for the nominal case and the smooth gradients case. Here it is seen that in the smooth gradients case, the emission profile is significantly broader in the Kα spectral region (upper plot). Specifically, the gap between "hot" and "cold" lines is almost completely filled by transitions from moderate and low ionizations. In addition, the level of emission from the Kβ spectral region (lower plot) is significantly higher in the smooth gradient case, and approaches the magnitude of the cold Kα line emission. Thus, the smooth gradient case, which has a larger amount of high temperature material in the mix region, is less consistent with the experimental data in Figure 1 than the simple 4-region case.

While the distributions used in this calculation were arbitrary and no attempt has been made to fit to experimental data, these results do show that both the Kα and Kβ spectral features can be significantly affected by the presence of gradients.

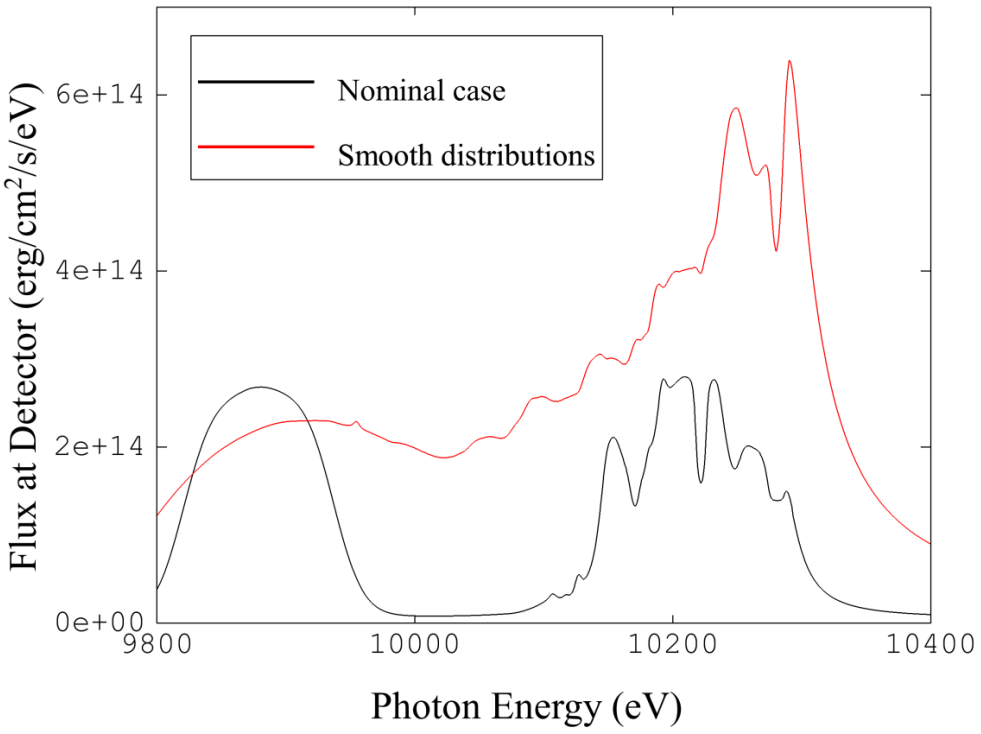

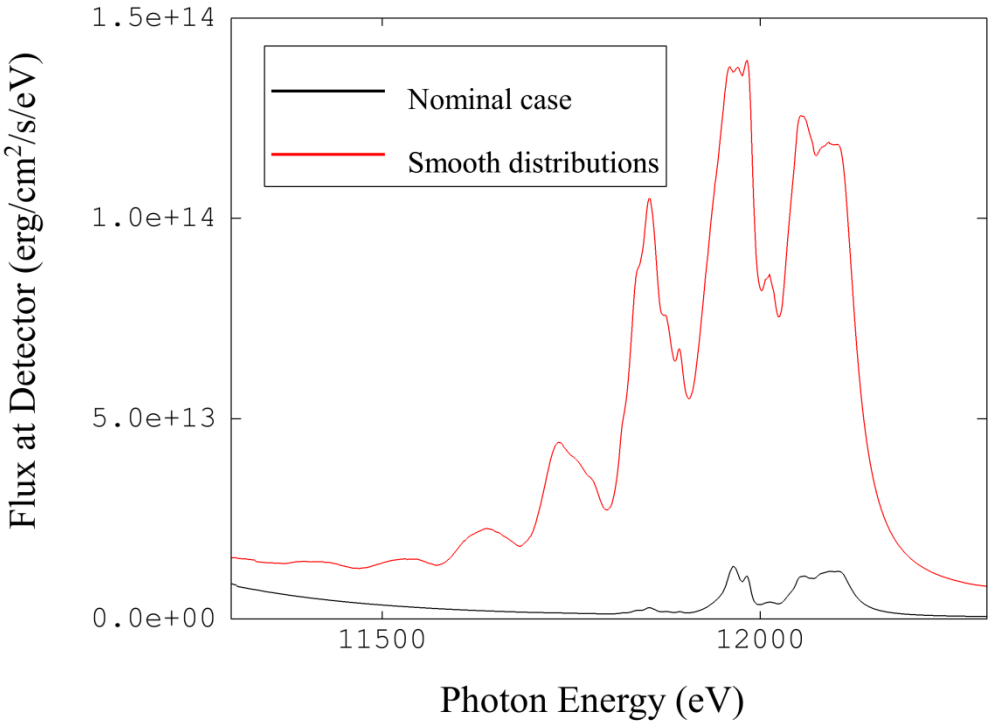

Figure 18. Comparison of calculated spectra for Ge Kα (top) and Kβ (bottom) transitions computed for nominal 4-region hot/cold mix case and the case with smoothly varying plasma distributions in mix region.

References

[1] S. P. Regan, *et al.,* "National Ignition Facility (NIF) Implosions: Hydrodynamic Mixing Experiments," 3rd International Conf. on High Energy Density Physics, Lisbon, Portugal, May 2011.

[2] P. Nilson, *et al.,* "Target Heating Effects on the $K_{\alpha 1,2}$ Emission Spectrum from Solid Targets Heated by Laser-Generated Hot Electrons, Phys. Plasmas **18**, 042702 (2011).

[3] J. J. MacFarlane, I. E. Golovkin, and P. R. Woodruff, "Modeling of Inner-Shell Kα and Kβ Line Emission from Cu Targets Heated by Short-Pulse Lasers", Prism Computational Sciences Report No. PCS-R-113, August 2010.